Study of the Ionospheric TEC Rate in Hong Kong Region and its GPS/GNSS Application

LIU Zhizhao, WU Chen

Dept of Land Surveying & Geo-Informatics, the Hong Kong Polytechnic University, Hung Hom, Kowloon, Hong Kong, China

e-mail: {lszzliu, lswuchen}@polyu.edu.hk

Abstract: This paper proposes the derivation of accurate ionospheric total electron contents (TEC) rate data using GNSS carrier phase measurements without the need of ambiguity resolution. The GNSS measurements collected at 30-second interval during an ionosphere quiet period (1-2 January 2009) and a severe ionosphere disturbance period (31 March to 1 April 2001) from the Hong Kong permanent GNSS network SatRef are used to implement this proposed method. The data analysis results show that the nominal slant TEC rate over Hong Kong, a low latitude region, is about 0.01 TECU/sec during ionosphere quiet periods and the nominal slant TEC rate in ionosphere disturbance periods is 0.03 TECU/sec—three times of TEC rate in ionosphere quiet periods. This paper also analyzes the application of the TEC rate information in the cycle slip detection and repair for the GPS/GNSS carrier phase measurements. The analysis shows that the use of this information is very effective in identifying even very small cycle slips (one cycle). This method is particularly useful in processing high rate GPS/GNSS observations e.g. real-time kinematic surveying. This paper also exemplifies the interesting and important coupling relationship between the GPS/GNSS and ionosphere research.

Keywords: GPS/GNSS; total electron content (TEC); ionospheric TEC rate; cycle slip

1 Introduction

The signals of the satellite-based navigation systems such as global positioning system (GPS) and global navigation satellite system (GNSS) transmit from satellites to receivers on or near the Earth and these signals inevitably experience ionosphere-induced error when passing through the ionosphere. The ionosphere-induced error is by far the largest one in satellite-based positioning and navigation (Allain and Mitchell, 2009). To obtain high precision such as centimeter level positioning solution with GPS/GNSS, the ionosphere-induced error must be well studied and modeled. On the other hand due to the dispersive property of the ionosphere and the availability of multiple-frequency GPS/GNSS signals, the GPS/GNSS in turn is a very useful tool for the ionosphere studies. This coupling relationship between GPS/GNSS and ionosphere determines that the study of ionosphere using GPS/GNSS data is a significant topic for both GPS/GNSS and ionosphere research.

In the study of ionosphere, an important and frequently used variable to measure and quantify the ionosphere is the total electron contents (TEC) – a measure of the total number of free electrons in a one-squared meter column from the bottom to the top of the ionosphere. The ionospheric TEC is used to describe the ionosphere because it gives a quantitative measure of the total number of electron contents along the line of sight and because it can be easily derived from dual-frequency GPS/GNSS data. In the past, the study of TEC using GPS/GNSS technology has been carried out by many efforts (Komjathy et al., 1998; Komjathy and Born, 1999; Skone, 2001; Mitchell and Spencer, 2003; Mannucci et al., 1999; Bilitza et al., 1999; Liu and Gao, 2005; Skone and Hoyle, 2005; Chen et al., 2008; Hernandez-Pajares et al., 2008). Comparatively, the study of the rate of TEC was less specifically focused although it has been reported in literatures (e.g. Skone and Hoyle, 2005; Chen et al., 2008). While the absolute value of the TEC is a very important parameter to represent the status of the ionosphere, the TEC rate is another important parameter that characterizes the dynamic change of the ionosphere. The ionospheric TEC rate is a relative quantity since it is only concerned with the TEC values of two consecutive epochs. While the TEC itself provides a measure of the magnitude of the ionospheric activities, the TEC rate provides a measure of the spatial and temporal correlation of the ionospheric activities (Wanninger, 1993; Stewart and Langley, 1999; Pi et al., 1997).

When using GPS/GNSS carrier phase measurements, the derivation of TEC rate is comparatively easier and more accurate than derivation of TEC. Since the TEC rate is related with only two consecutive epochs, the GPS/GNSS carrier phase measurements can be easily employed to de-

978-1-935068-03-7

rive the TEC rate without the necessity of resolving the carrier phase ambiguities. When the measurements of two adjacent epochs are used, the constant carrier phase ambiguity can be cancelled. Even if the frequently encountered cycle slip problem occurs, it will be easily detected and corrected based on the existing information. The cycle slip detection and correction method will be elaborated more in the paper later. For the study of TEC, the ambiguities of the carrier phase measurements must be resolved in order to derive the absolute value of TEC. Currently, the correct resolution of carrier phase ambiguity is still not a guaranteed work although significant progresses have been made in the past decades (Wei and Schwarz, 1995; Teunissen, 1999; Ge et al., 2008; Feng, 2008; Teunissen and Verhagen, 2008). From this point of view, the TEC rate values should be more precise than the TEC data since they are not affected by potential ambiguity resolution error or cycle slip.

This study will focus on the analysis of the GPS data in Hong Kong region. Hong Kong is located at the low latitude region (geomagnetic latitude 12 degrees North) (Chen et al., 2008). The GNSS observations at low latitude regions are particularly affected by the ionosphere (Vladimer et al., 1999). The GNSS is widely accepted and used in Hong Kong. In Hong Kong's aviation industry alone, the survey indicated that about 80% of the aircrafts to/from Hong Kong are equipped with GNSS equipment and this percentage was expected to increase (APEC, 2004). With the installation of GNSS satellite network (SatRef), much of the landing surveying work is done using the GNSS technology. Considering the multiple factors, e.g. the severe ionospheric effect due to its low latitude, and the wide application of GNSS technology including the safety critical aviation industry, the study of ionosphere in Hong Kong becomes a particularly important research subject for the GPS/ionosphere researchers.

2 Method of Deriving TEC Rate from Carrier Phase Data

This section presents the method of deriving the ionospheric TEC rate from dual-frequency GNSS data. With the carrier phase measurements recorded at two frequencies, the carrier phase based TEC can be computed as (Liu et al., 2005):

$$TEC_j = \frac{f_1^2[(\lambda_1 j_1 - \lambda_2 j_2) - (\lambda_1 N_1 - \lambda_2 N_2) - b_i - bp]}{40.3 \times 10^{16}(y-1)} \qquad (1)$$

where TEC_Φ is the TEC derived from carrier phase measurements, in unit of TECU; f_1 is the frequency of the L1 frequency, in unit of Hz; Φ_1 and Φ_2 are the carrier phase measurements on L1 and L2 frequencies respectively, in unit of cycle; λ_1 and λ_2 are the wavelength of L1 and L2 frequencies respectively, in unit of meter/cycle; N_1 and N_2 are the integer ambiguities of measurements Φ_1 and Φ_2 are the carrier phase measurements on L1 and L2 frequenc respectively, in unit of cycle; b_i bp and b^p are the receiver inter-frequency bias and satellite inter-frequency bias, respectively, in unit of meter; v is the squared ratio between the frequencies of L1 and L2, $v=(f_1/f_2)^2$. To get the absolute TEC_Φ are value, the carrier phase ambiguities N_1 and N_2 in Eq. (1) must be first determined. The precise determination of the ambiguities is still a challenge although significant progress has been made in the past decades. Therefore the direct calculation of $TEC_\Phi$is still not an easy work and the TEC rate subsequently cannot be calculated directly. Considering the invariability property of the ambiguities during a continuous signal tracking when the signals are free from cycle slips, the epoch-wise differencing method can be employed to derive the TEC rate. Assuming that at two consecutive epochs t_i and t_{i-1} , the TEC_Φ are computed following Eq. (1), the TEC rate at epoch t_i thus can be readily derived as:

$$TECR_\phi(t_i) = \frac{TEC_\phi(t_i) - TEC_\phi(t_{i-1})}{t_i - t_{i-1}} \qquad (2)$$

If the TEC rate calculation is performed in post-mission, a more accurate TEC rate can be derived using the TEC data one epoch prior to and post- the current epoch to determine the TEC rate at current epoch. Thus the Eq. (2) can be slightly modified as:

$$TECR_\phi(t_i) = \frac{TEC_\phi(t_{i+1}) - TEC_\phi(t_i)}{2(t_{i+1} - t_i)} + \frac{TEC_\phi(t_i) - TEC_\phi(t_{i-1})}{2(t_i - t_{i-1})} \qquad (3)$$

Normally the interval between the consecutive epochs is the same (i.e. $t_{i+1} - t_i = t_i - t_{i-1} = \Delta t$), Eq. (3) can be further simplified as:

$$TECR_\phi(t_i) = \frac{TEC_\phi(t_{i+1}) - TEC_\phi(t_i)}{2\Delta t} + \frac{TEC_\phi(t_i) - TEC_\phi(t_{i-1})}{2\Delta t} = \frac{TEC_\phi(t_{i+1}) - TEC_\phi(t_{i-1})}{2\Delta t} \qquad (4)$$

Substituting Eq. (1) for TEC terms at the right hand side of Eq. (4), the following Eq. (5) can be obtained:

$$
\begin{aligned}
\mathrm{TECR}_{\phi}(\mathrm{t_i}) &= \frac{\mathrm{TEC}_{\phi}(\mathrm{t_{i+1}})-\mathrm{TEC}_{\phi}(\mathrm{t_{i-1}})}{2\Delta t} \\
&= \frac{f_1^2}{40.3\times10^{16}(\mathrm{y}-1)\times 2\Delta \mathrm{t}}\{[(\lambda_1\phi_1(\mathrm{t_{i+1}})-\lambda_2\phi_2(\mathrm{t_{i+1}})) \\
&\quad -(\lambda_1 N_1(\mathrm{t_{i+1}})-\lambda_2 N_2(\mathrm{t_{i+1}}))-b_1(\mathrm{t_{i+1}})-\mathrm{b^p}(\mathrm{t_{i+1}})] \\
&\quad -[(\lambda_1\phi_1(\mathrm{t_{i-1}})-\lambda_2\phi_2(\mathrm{t_{i-1}})) \\
&\quad -(\lambda_1 N_1(\mathrm{t_{i-1}})-\lambda_2 N_2(\mathrm{t_{i-1}}))-b_1(\mathrm{t_{i-1}})-\mathrm{b^p}(\mathrm{t_{i-1}})]\}
\end{aligned} \tag{5}
$$

Since the ambiguities N_1 and N_2 are invariable over time if they are free of cycle slips and the biases b_i and b^p are nearly constant over such a period as short as Δt (Δt normally does not exceed a few minutes), the Eq. (5) can be rewritten as:

$$
\begin{aligned}
\mathrm{TECR}_{\phi}(\mathrm{t_i}) &= \frac{\mathrm{f_1^2}}{40.3\times10^{16}(\mathrm{y}-1)\times 2\Delta \mathrm{t}}\{[(\lambda_1\phi_1(\mathrm{t_{i+1}}) \\
&\quad -\lambda_2\phi_2(\mathrm{t_{i+1}}))-[(\lambda_1\phi_1(\mathrm{t_{i-1}})-\lambda_2\phi_2(\mathrm{t_{i-1}}))]\} \\
&= \frac{\mathrm{f_1^2}}{40.3\times10^{16}(\mathrm{y}-1)\times 2\Delta \mathrm{t}}\{\lambda_1(\phi_1(\mathrm{t_{i+1}})-\phi_1(\mathrm{t_{i-1}})) \\
&\quad -\lambda_2(\phi_2(\mathrm{t_{i+1}})-\phi_2(\mathrm{t_{i-1}})]\}
\end{aligned} \tag{6}
$$

From Eq. (6), it can be seen that the carrier phase based TEC rate can be calculated even if the ambiguities and inter-frequencies biases are unknown. Unlike the derivation of the TEC data as in Eq. (1), the ambiguities and inter-frequency biases don't affect the TEC rate derivation at all and the resolution of them is completely unnecessary. This is obviously an advantage of using TEC rate over using TEC data to describe the ionosphere.

3 Data Analysis

The data used in the analysis are obtained from the Hong Kong SatRef network. The SatRef is a permanent network consisting of 12 Continuously Operating Reference Stations (CORS) that were developed by the Lands Department of Government of Hong Kong Special Administrative Region (HKSAR).

Two datasets are analyzed in this paper. One dataset was collected during 1-2 January 2009, which corresponds to an ionosphere quiet period. The geomagnetic Kp index of this dataset is illustrated in Figure. The three GNSS stations, HKFN, HKMN and HKOH, in the SatRef network are selected for this dataset analysis and they are depicted in the Figure. The distribution of the three stations basically covers the whole Hong Kong region and fairly represents the ionospheric condition of the each district in Hong Kong region. The second dataset was collected during 31 March to 1 April 2001, which represents a time with severe ionospheric disturbances and of which the Kp index is plotted in Figure. Figure and Figure clearly indicate that the ionospheric conditions of the two datasets are

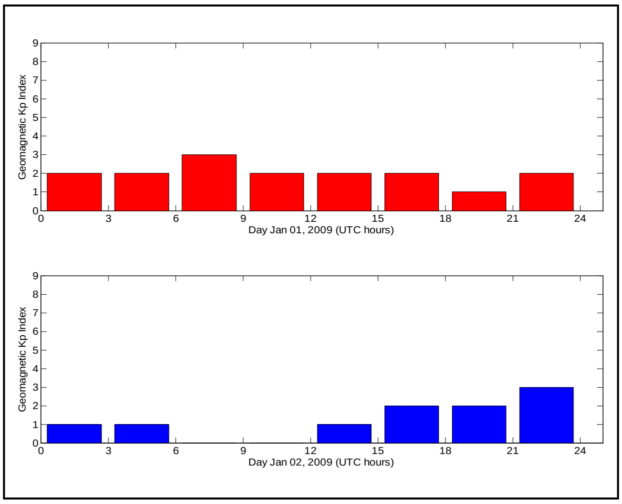

Figure 1. Geomagnetic Kp index for Jan. 1-2, 2009

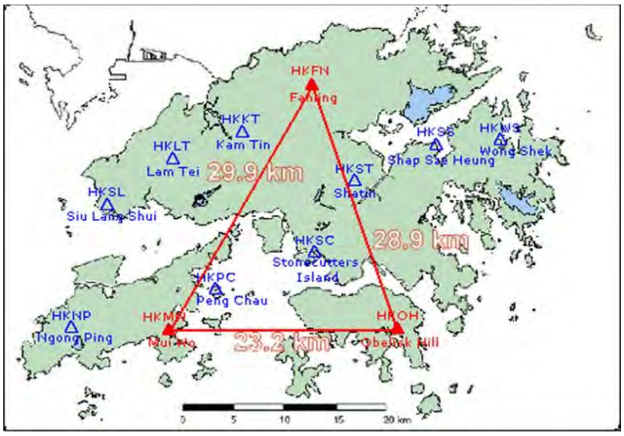

Figure 2. The selected GNSS stations in the SatRef

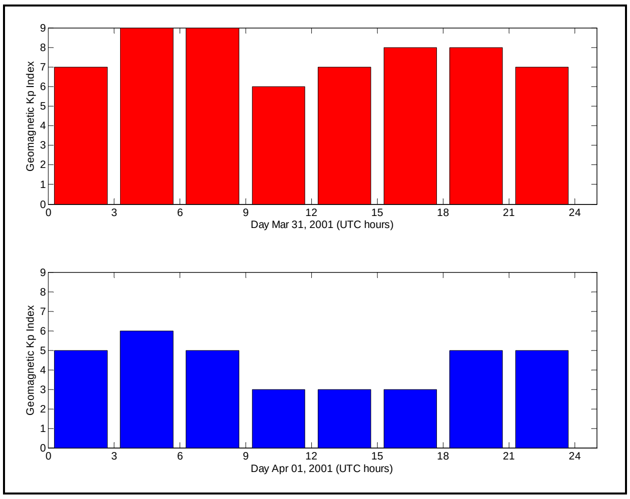

Figure 3. Geomagnetic Kp index for March 31-April 1, 2001

significantly different. This paper exactly intends to study the TEC rate information of Hong Kong region under various ionospheric conditions – both quiet and active.

The GNSS data collected by the SatRef network are recorded at an interval of 30 seconds. During the data analysis, this interval of 30 seconds is kept unchanged and cutoff angle of 15 degrees is used. Although both GPS and GLONASS observations are available in the data files of the SatRef network, only the GPS data are analyzed in this paper considering the quality of the GPS data are much more stable and accurate than that of GLONASS data. It should be mentioned that the TEC rate calculated with Eq. (6) is a quantity in the slant direction. No mapping function is used in this study to project the slant TEC rate to the zenith direction. The use of slant TEC rate has two benefits. One is that it eliminates the uncertainty brought by the mapping function. Second, this slant TEC rate can be directly used in GPS/GNSS cycle slip detection and repair, as to be discussed in the following section, without any further reduction. If zenith TEC rate is derived, it has to be converted into slant direction when it is used in assisting GPS/GNSS cycle slip detection and repair.

3.1 TEC Rate Results of Quiet Ionosphere

This section presents the results obtained from the dataset one that was collected during the quiet ionosphere condition. The two-day GPS-derived TEC rate results for the three stations are presented in Figure 4 to Figure 9. In each figure, the y-axis represents the TEC rate, the x-axis denotes the UTC time and local time. The top row of numbers is the UTC hours and the bottom row of numbers is the local time hours. The slant TEC rates observed by each individual satellite are represented by different colors and different symbols in each figure. The six figures show that under quiet ionosphere condition, the TEC rates observed by all the satellites at all the three stations are about 0.01 TECU/sec during the 48-hour data session. These six figures demonstrate that the ionosphere over the entire Hong Kong region is very stable during the ionosphere quiet periods. The only slight TEC rate perturbation occurs slightly before 11 hour local time but this perturbation is very small and only observed by a few satellites. Generally the ionospheric structure of Hong Kong on the quiet period is very stable spatially (in every azimuth) and temporally. The TEC rate of 0.01 TECU/sec means that, if the GNSS data

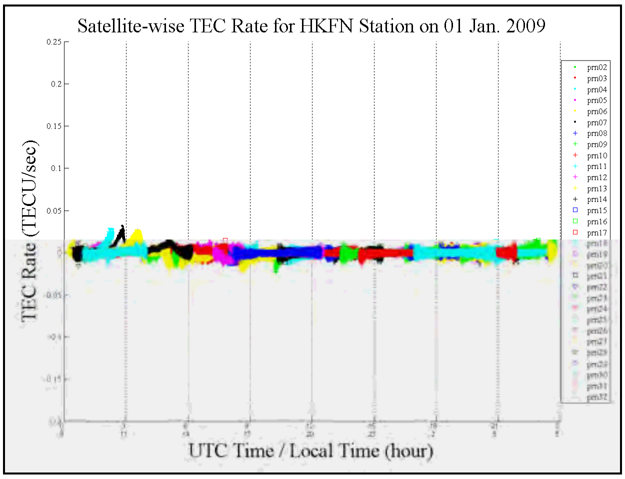

Figure 4. The GPS-derived TEC rate observed at HKFN station on 1st January 2009

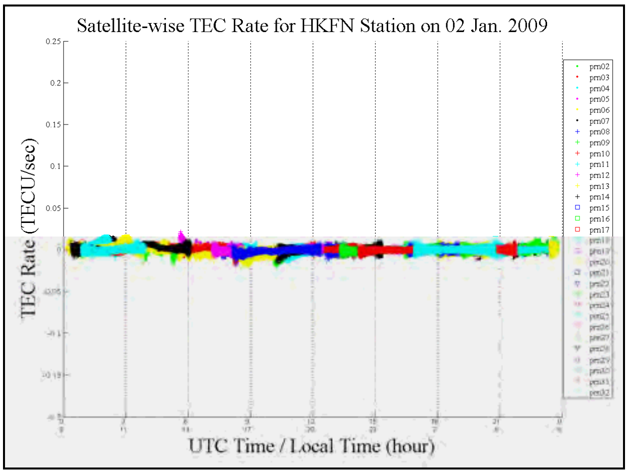

Figure 5. The GPS-derived TEC rate observed at HKFN station on 2nd January 2009

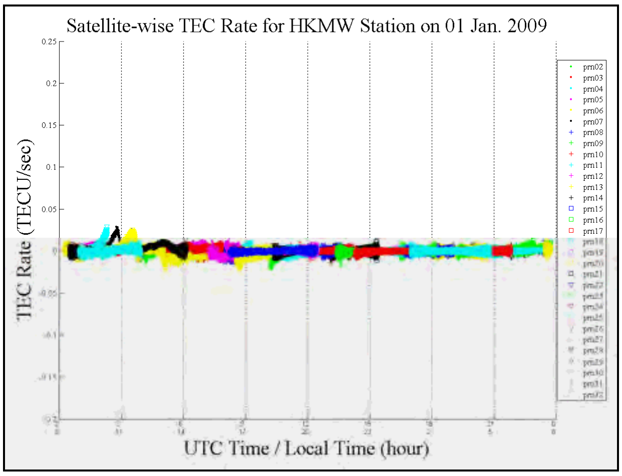

Figure 6. The GPS-derived TEC rate observed at HKMW station on 1st January 2009

are recorded at a rate of 1 Hz, the TEC change between two consecutive epochs will be about 0.01 TECU – translating into distance of 1.6 mm on GPS L1 signal. When the data

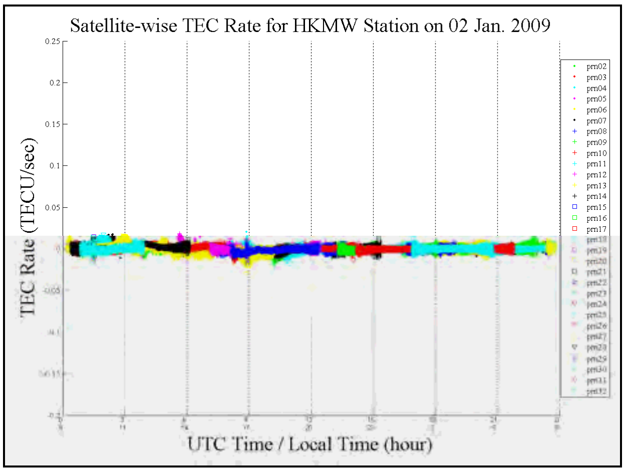

Figure 7. The GPS-derived TEC rate observed at HKMW station on 2nd January 2009

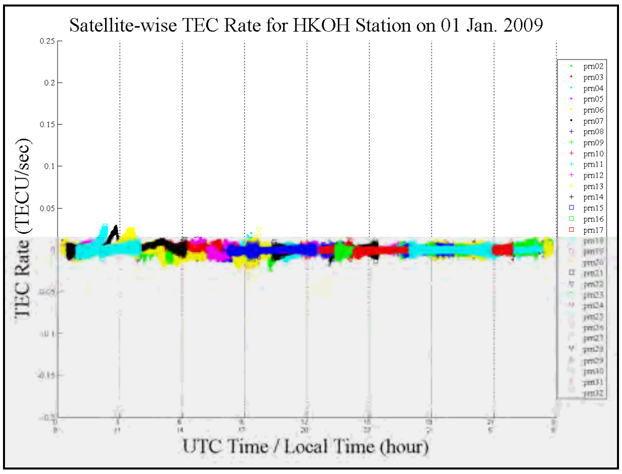

Figure 8. The GPS-derived TEC rate observed at HKOH station on 1st January 2009

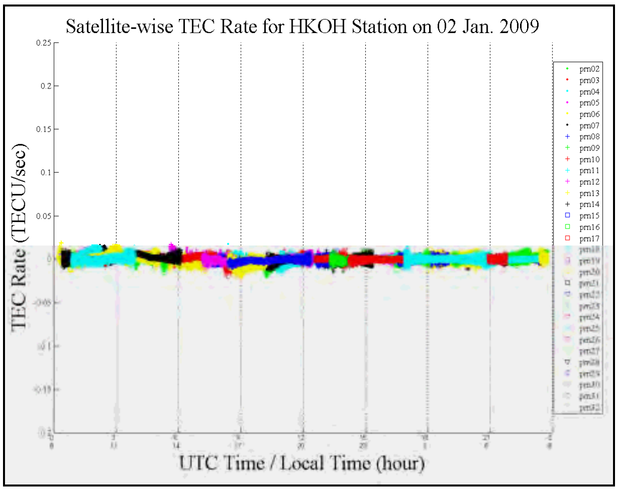

Figure 9. The GPS-derived TEC rate observed at HKOH station on 2nd January 2009

are recorded at an interval of 30 seconds, the epoch-by-epoch TEC change will be approximately 0.3 TECU – equivalent to 4.9 cm in distance on GPS L1 signal. This TEC change is well smaller than the wavelength of the L1 signal (19 cm), thus it will be easy to distinguish carrier phase cycle slip from TEC change. It will be shown later in this paper this representative TEC rate, 0.01 TECU/sec, is a very useful threshold for pre-processing and cleaning the GNSS data at Hong Kong region on ionospheric quiet days.

3.2 TEC Rate Results of Active Ionosphere

On the 31 March 2001, a severe geomagnetic storm occurred (Foster et al., 2002). On this day the Kp index reached the highest level of 9, as depicted in the top panel of Figure. On 1st April 2001, the geomagnetic storm became weaker than the previous day but its Kp index was still as high as 5~6, as indicated in the bottom panel of Figure. These two days represent a typical active ionosphere situation. The section's analysis of the SatRef data will give us a representative measure of the TEC rate in Hong Kong during ionosphere active period. Please note that HKMW and HKOH stations used in the first dataset are not used here. This is because there was no data collection at these two stations in 2001.

The following Figure 10 to Figure 15 illustrate the satellite-wise TEC rates for three stations (HKFN, HKKT, HKKY) over the geomagnetic storm period. Compared to the results of ionosphere quiet period shown in dataset one, the TEC rates of this dataset are significantly larger. It is common for satellites to have TEC rate of 0.05 TECU/sec, which is nearly 5 times higher than that during ionospheric quiet period. For some satellites such as PRN 28 on 31 March at about 23 UTC, the TEC rate can even be as high as 0.15~0.20 TECU/sec. Due to the effect of this severe geomagnetic storm, the GPS signals suffered outages during the observations, e.g. slightly before 12 UTC at the three stations, as confirmed by Figure 10 to Figure 12. During the 02~08 UTC, the main storm phase was present when the northward interplanetary magnetic field (IMF) turned south, neglecting occasional of reverse in which the IMF returned to north (Metatech, 2001). Please note commencing approximately at 02 UTC, the IMF turned south. But it then turned north again. At about 03 UTC, the IMF turned south with larger value of Bz component of the IMF than at 02 UTC. Therefore, in this paper the southbound Bz commencement line is marked at 03 UTC.

978-1-935068-03-7 © 2009 SciRes.

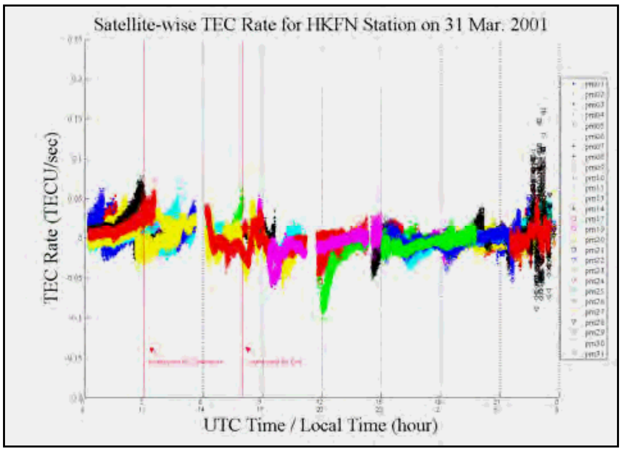

Figure 10. The GPS-derived TEC rate observed at HKFN station on 31 March 2001

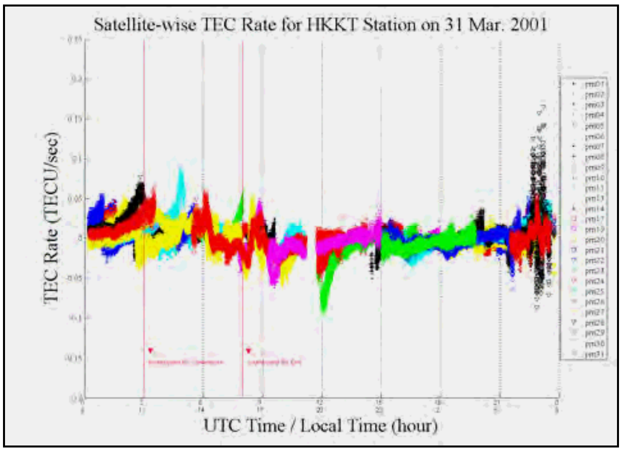

Figure 11. The GPS-derived TEC rate observed at HKKT station on 31 March 2001

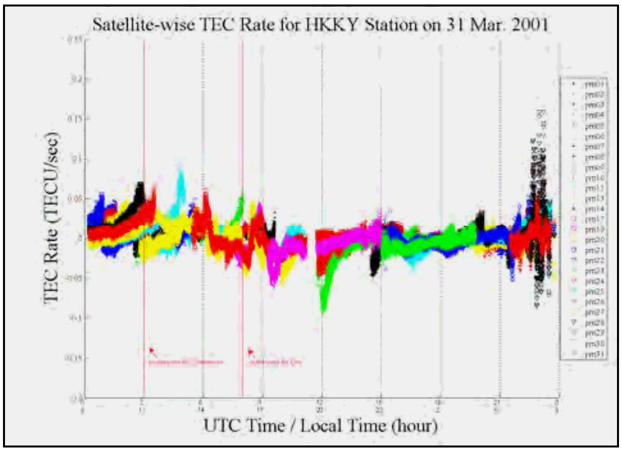

Figure 12. The GPS-derived TEC rate observed at HKKY station on 31 March 2001

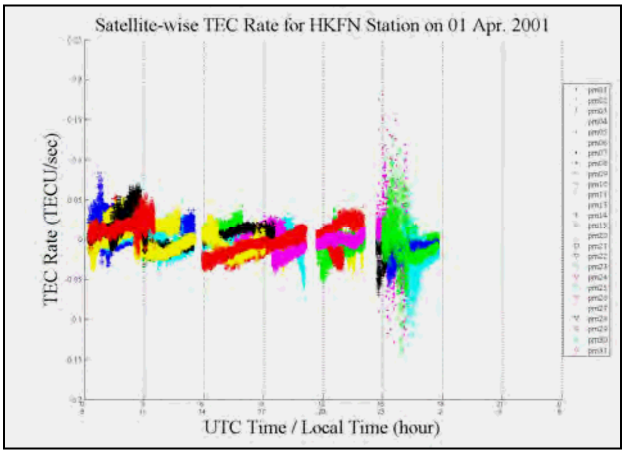

Figure 13. The GPS-derived TEC rate observed at HKFN station on 1 April 2001

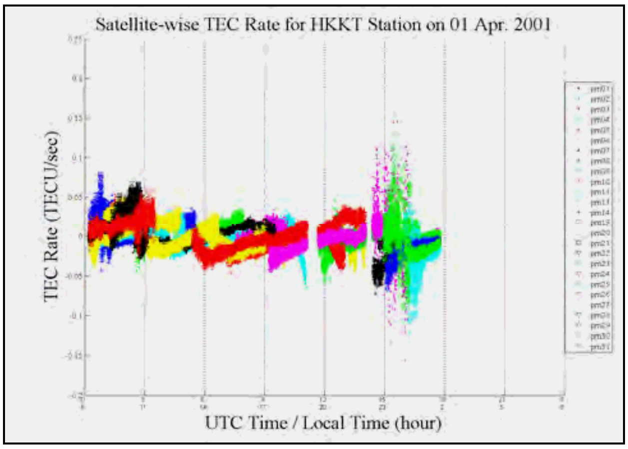

Figure 14. The GPS-derived TEC rate observed at HKKT station on 1 April 2001

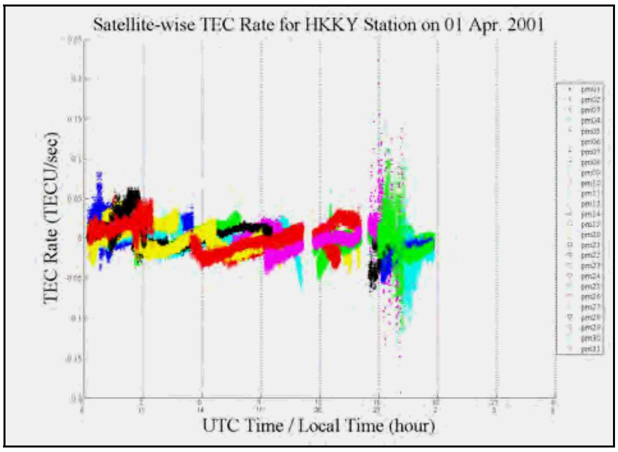

Figure 15. The GPS-derived TEC rate observed at HKKY station on 1 April 2001

During the main storm period (03~08 UTC), the TEC rates observed at the three stations in Hong Kong do not show particularly large disturbances, although an apparent increase of the amplitude of the TEC rates occurs around 03 UTC. Figure 10 to Figure 12 reveal that the TEC rates have a large perturbation approximately at 7h local time 1 April, which obviously results from a perturbation of the ionosphere. It is observed in Figure 13 to Figure 15 that approximately at 23h local time 1 April, the measured TEC rates have a marked increase. This might be caused by the anomalous increase of the ionization density in E-region in the low and middle latitudes (Bauske et al., 1997).

3.3 Statistics of the TEC Rate Results

The statistics of all satellites' TEC rates observed from the two datasets are illustrated in Figure 16 and Figure 19. Figure 16 and Figure 17 show the daily satellite-wise mean TEC rates tracked by each station for the quiet and disturbed ionospheric datasets, respectively. Figure 16 clearly shows that the mean TEC rate of all the satellites observed in Hong Kong region is well bounded within 0.01 TECU/sec when the ionosphere is in quiet condition. Figure 16 also indicates that each satellite's mean TEC rate has a very good day-to-day, station-to-station repeatability. Not only do the 1 January and 2 January mean TEC rates agree very well on each individual station, but also they agree consistently among the three stations. For the disturbed ionosphere dataset, Figure 17 noticeably shows that the TEC rates are significantly larger than those in the quiet ionosphere period. The amplitude of the TEC rate variation is as large as 0.03 TECU/sec, which is about 3 times of that in Figure 16. The TEC rates also show much larger variability among different satellites, compared to that of Figure 16. This apparently results from the large temporal and spatial ionosphere disturbances due to the geomagnetic storm. The Figure 17 indicates that for the same satellite, the TEC rates observed from three stations have a very good agreement – implying that the ionospheric spatial correlation among the ground receivers are still quite strong but the spatial correlation among the space satellites are weak, as evidenced by the scattered TEC rate of each satellite.

The standard deviations (STD) of the TEC rates for the two datasets are presented in Figure 18 and Figure 19, respectively. Figure 18 shows that the TEC rate STDs of all the satellites are well below 0.01 TECU/sec. Similar to the mean TEC rates, each satellite's TEC rate STD on the quiet ionosphere period is very consistent from day to day, from station to station. The TEC rate STD of each satellite is also quite comparable with each other, with only relatively large STDs on several satellites such as PRN 7, PRN 8, PRN 27 and PRN 28. For the ionosphere disturbance period, the magnitude of the TEC rate STD increases significantly from the 0.01 TECU/sec at quiet period to nearly 0.03 TECU/sec. The STDs of different the satellites scatter significantly as shown in Figure 19. But the daily STDs of each satellite generally have only little variation among three stations – again indicating that the spatial correlation among the ground receivers is strong.

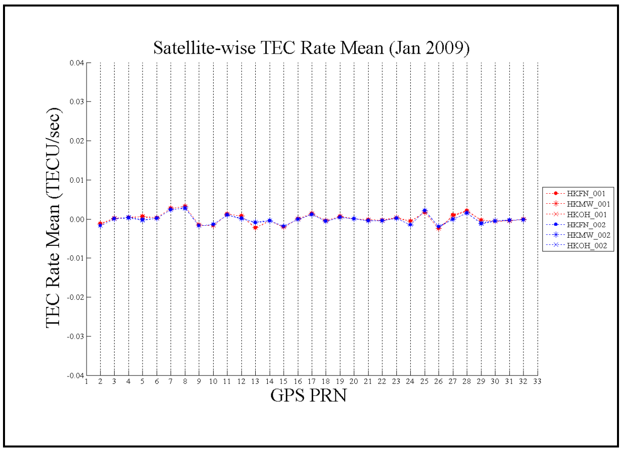

Figure 16. The satellite-wise mean TEC rate at three stations during 1-2 January 2009

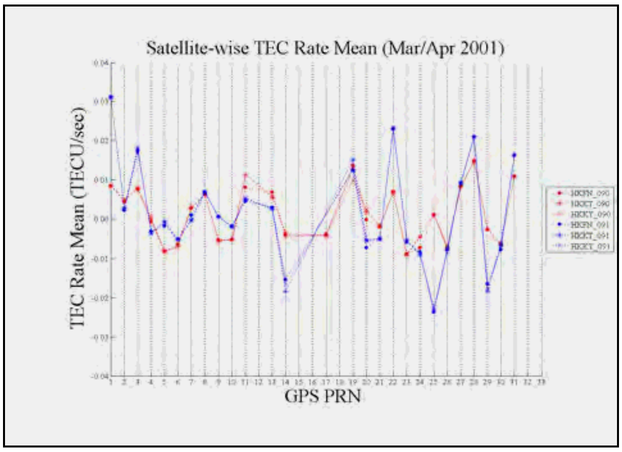

Figure 17. The satellite-wise mean TEC rate at three stations during 31 March-1 April 2009

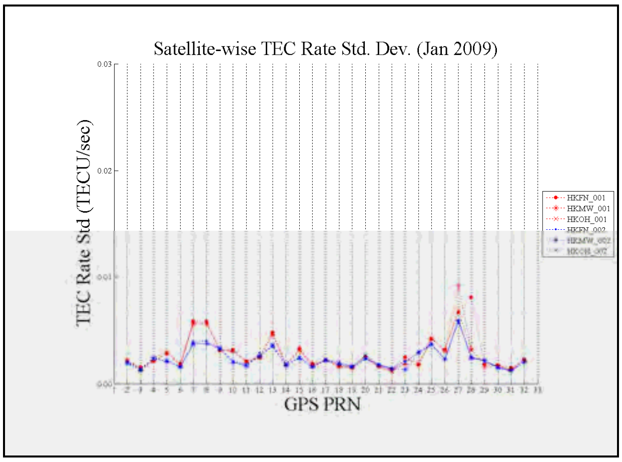

Figure 18. The satellite-wise TEC rate standard deviation at three stations during 1-2 January 2009

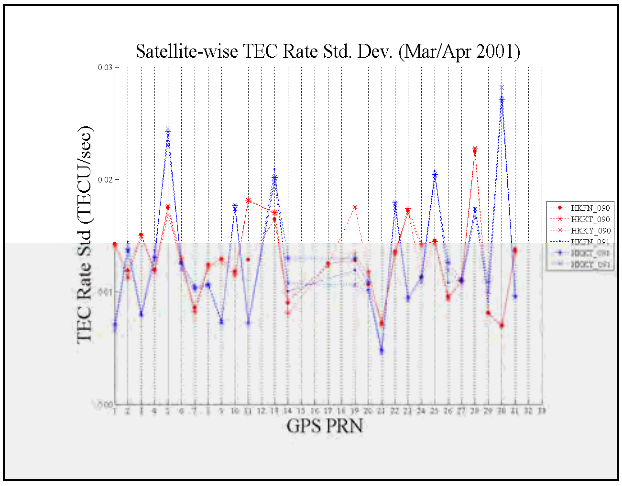

Figure 19. The satellite-wise TEC rate standard deviation at three stations during 31 March-1 April 2009

4 Application of TEC Rate in GPS/GNSS

As shown above, the TEC rate is accurately derived from GPS/GNSS carrier phase measurements. Once the TEC rate is obtained, this information can become useful in GPS/GNSS applications for assisting GPS/GNSS data cleaning. In the handling of GPS/GNSS carrier phase measurements, one of the important tasks is to detect and repair cycle slips. The presence of undetected or unrepaired cycle slips in the carrier phase measurements will result in a significant amount of extra work in the ambiguity resolution and make the already complex ambiguity resolution problem even more complicated. Therefore the effective detection and repair of the cycle slips are always a fundamental task in GPS/GNSS carrier phase processing.

Assuming that there are cycle slips on GPS L1 and L2 frequencies at epoch $t_{i=1}$, denoted as δN_1 and δN_2 respectively, the TEC rate that is affected by cycle slips therefore can be derived as below, based on Eq. (6):

$$\mathrm{TECR}_j(t_i)=\frac{f_1^2}{40.3\times10^{16}(y-1)\times2\Delta t}\{\lambda_1(j_1(t_{i+1})+\delta N_1-j_1(t_{i-1}))-\lambda_2(j_2(t_{i+1})+\delta N_2-j_2(t_{i-1})]\} \quad (7)$$

Please note in Eq. (6), in order to derive a more accurate TEC rate at epoch t_i in the post-mission mode, two epochs of data adjacent to t_i are used. In the cycle slip detection, only the data prior to epoch t_i is necessary. Therefore the Eq. (7) can be modified as:

$$\mathrm{TECR}_\phi(t_i)=\frac{f_1^2}{40.3\times10^{16}(y-1)\times\Delta t}\{\lambda_1(\phi_1(t_i)+\delta N_1-\phi_1(t_{i-1}))-\lambda_2(\phi_2(t_i)+\delta N_2-\phi_2(t_{i-1})]\} \quad (8)$$

With Eq. (8) it can be estimated that one cycle of slip on L1 frequency will result in a change of 0.0604 TECU/sec in TEC rate, when the Δt=30*sec* and there is no cycle slip on L2 frequency. Similarly when $\delta N_1=0$ and there is one cycle of slip on L2 frequency ($\delta N_2=1$ or $\delta N_2=-1$), the resultant TEC rate change is 0.0775 TECU/sec. When both δN_1 and δN_2 have one cycle of slip of same sign, the TEC rate change will be 0.0171 TECU/sec. When both δN_1 and δN_2 have one cycle of slip but of opposite sign, the TEC rate change will be 0.13795 TECU/sec. In the implementation of cycle slip detection, the TEC rate is first calculated using Eq. (8) with both $\delta N_1=0$ and $\delta N_2=0$, assuming that there is no cycle slip on either L1 or L2 frequencies. When the magnitude of the computed TEC rate exceeds the nominal TEC rate values (e.g. in Hong Kong, on ionosphere quiet period 0.01 TECU/sec, and on ionosphere disturbance period 0.03 TECU/sec), it indicates that it is very likely there are cycle slips on either L1 or L2 or both frequencies. Once the cycle slip is detected, its size can be searched until the calculated TEC rate is smaller than or equal to the nominal ionospheric TEC rate. It should be noted that there are some special pairs of cycle slips on L1 and L2, with which the TEC rate may have very little or even no change. For instance when $\delta N_1=77$ and $\delta N_2=60$, the TEC rate calculated from Eq. (8) will be identical as that when $\delta N_1=0$ and $\delta N_2=0$. For these special cases, other approaches have to be used together with this one to effectively detect and repair cycle slips. It should be noted that in the above demonstration of the impact of cycle slip on TEC rate, the GPS/GNSS data interval is assumed to be 30 seconds. In real-time applications where short interval is normally used (e.g. Δt=1*sec*), the effectiveness of using ionospheric TEC rate information to detect cycle slip will become more prominent because the TEC rates calculated above will become 30 times larger. For instance, the change of TEC rate will become 1.8124 TECU/sec when δN_1=1 or δN_1= –1 and δN_2=0. Such a high level of TEC rate is approximately 60 times higher than the nominal TEC rate during ionosphere disturbance period. Therefore, the identification of cycle slip in the carrier phase measurements will become much easier, compared to larger observation interval (e.g. 30 seconds). This indicates that using the TEC rate information as a threshold to detect cycle slip is a very effective, although not exclusive, approach in the GPS/GNSS data cleaning.

5 Conclusions

This paper proposes the derivation of accurate TEC rate data using GNSS carrier phase measurements without the need of ambiguity resolution. This proposed method is implemented using the Hong Kong SatRef network GPS data recorded at 30-second interval and the knowledge of the TEC rate over Hong Kong region is obtained. The analysis of the data collected in the ionosphere quiet period reveals that the ionospheric slant TEC rate is well below 0.01 TECU/sec in terms of both mean value and standard deviation. During severe ionosphere disturbance period, both mean and standard deviation of the slant TEC rates observed at Hong Kong can be as large as 0.03 TECU/sec, approximately 3 times larger than the ionosphere quiet time.

This paper also analyzes the application of the TEC rate information in the cycle slip detection and repair for the GPS/GNSS carrier phase measurements. It shows that the use of this information is very effective in identifying even very small cycle slips (one cycle). This method is particularly useful in high rate GPS/GNSS observations e.g. real-time kinematic surveying.

6 Acknowledgments

The first author would like to thank Prof. Xiaoli Ding, Dr. Lilian Shuk-ching PUN CHENG, and the Department of Land Surveying and Geo-Informatics, The Hong Kong Polytechnic University for fully supporting the trip to the conference. The Lands Department of the Government of Hong Kong Special Administrative Region (HKSAR) is thanked for providing observation data from the Hong Kong Satellite Positioning Reference Station Network (SatRef).

References

[1] Allain D. J., C. N. Mitchell (2009) Ionospheric delay corrections for single-frequency GPS receivers over Europe using tomographic mapping, GPS Solut, 13:141–151, DOI 10.1007/s10291–008–0107–y.

[2] APEC(2004),http://www.apecgit.org/meetings/meetings_51.asp?id=5, accessed on July 19, 2009.

[3] Bauske R., S. Noël, G. W. Prölss (1997) Ionospheric storm effects in the nighttime E region caused by neutralized ring current particles, Ann. Geophysicae, 15, pp. 300–305.

[4] Bilitza D., M. Hernandez-Pajares, J. M. Juan, J. Sanz (1999) Comparison between IRI and GPS-IGS derived electron content during 1991-1997, Physics and Chemistry of the Earth, Part C: Solar, Terrestrial & Planetary Science, 24(4), pp. 311-319

[5] Chen W., S. Gao, C. W. Hu, Y. Q. Chen, X. L. Ding (2008) Effects of ionospheric disturbances on GPS observation in low latitude area, GPS Solut, 12:33–41, DOI 10.1007/s10291–007–0062–z.

[6] Feng Y. (2008) GNSS three carrier ambiguity resolution using ionosphere-reduced virtual signals, Journal of Geodesy, 82(12).

[7] Foster J. C., P. J. Erickson, A. J. Coster, J. Goldstein, F. J. Rich (2002) Ionospheric signatures of plasmaspheric tails, Geophys. Res. Lett., 29(13), 10.1029/2002GL015067.

[8] Ge M., G. Gendt, M. Rothacher, C. Shi, J. Liu (2008) Resolution of GPS carrier-phase ambiguities in Precise Point Positioning (PPP) with daily observations, Journal of Geodesy, 82(7).

[9] Hernandez-Pajares M., J. Juan, J. Sanz, R. Orus, A. Garcia-Rigo, J. Feltens, A. Komjathy, S. Schaer, A. Krankowski (2008) The IGS VTEC maps: a reliable source of ionospheric information since 1998, Journal of Geodesy, 83(3/4), pp. 263–275.

[10] Komjathy A., G. H. Born (1999) GPS-based ionospheric corrections for single frequency radar altimetry, Journal of Atmospheric and Solar-Terrestrial Physics, 61(16), pp. 1197–1203.

[11] Komjathy A., R. B. Langley, D. Bilitza (1998) Ingesting GPS-derived TEC data into the International Reference Ionosphere for single frequency radar altimeter ionospheric delay corrections, Advances in Space Research, 22(6), pp. 793-801

[12] Liu Z. Z., Y. Gao (2005) Development and Analysis of a New 3D Ionospheric Modeling Method, *Navigation*, Journal of The Institute of Navigation, 51(4), pp. 311–329.

[13] Liu Z. Z., Y. Gao, S. Skone (2005) A study of smoothed TEC precision inferred from GPS measurements, Earth Planets Space, 57, pp. 999–1007.

[14] Mannucci A.J., B. Iijima, L. Sparks, X. Q. Pi, B. Wilson, U. Lindqwister (1999) Assessment of global TEC mapping using a three-dimensional electron density model, Journal of Atmospheric and Solar-Terrestrial Physics, 61(16), pp. 1227–1236.

[15] Metatech (2001) http://www.metatech-aps.com/Advisory/2001/Solar_GeomagAdvisory04_02.pdf, accessed on July 21, 2009.

[16] Mitchell C. N., P. S. J. Spencer (2003) A three-dimensional time-dependent algorithm for ionospheric imaging using GPS, Annals of Geophysics, 46 (4), pp. 687–696.

[17] Pi X., A. J. Mannucci, U. J. Lindqwister, C. M. Ho (1997) Monitoring of global ionospheric irregularities using the worldwide GPS network, Geophys Res Lett, 24(18), pp. 2283–2286.

[18] Skone S. H. (2001) The impact of magnetic storms on GPS receiver performance 75(9-10), pp. 457-468.

[19] Skone S., V. Hoyle (2005) Canadian GPS Network for Ionosphere Monitoring (CANGIM), GPS Solut, 9:59–62, DOI 10.1007/s10291-004-0117–3.

[20] Stewart P. J., R. B. Langley (1999) Monitoring the auroral oval with GPS and applications to WAAS, In: Proceedings of the ION 55th annual meeting, Cambridge,28-30 June 1999.

[21] Teunissen, P. J. G. (1999) GPS Ambiguity resolution as a classification problem, Studia Geophysica et Geodaetica, 43(1), pp. 61–72.

[22] Teunissen P. J. G., S. Verhagen (2008) GNSS Carrier Phase Ambiguity Resolution: Challenges and Open Problems, In International Association of Geodesy Symposia: "Observing our changing earth," (Ed.) M. Sideris, 133: 785–792, Springer.

[23] Vladimer J. A., P. Jastrezebeski, M. C. Lee, P. H. Doherty, D. T. Decker, D. N. Anderson, (1999) Longitude structure of ionospheric total electron content at low latitudes measured by TOPEX/Poseidon satellite, Radio Sci., 34, pp. 1239–1260.

[24] Wanninger L. (1993) Ionospheric monitoring using IGS data, In: Proceedings of the 1993 IGS workshop, Berne, 25–26, March 199.

[25] Wei M., K. P. Schwarz (1995) Fast ambiguity resolution using an integer nonlinear programming method, Proc. of ION GPS-1995, Palm Springs CA, pp. 1101–1110.

 978-1-935068-03-7